

DESIGN OF THE DIE PROFILE FOR THE INCREMENTAL RADIAL FORGING PROCESS*

M. AFRASIAB¹, H. AFRASIAB^{2**}, M.R. MOVAHHEDY³ AND G. FARAJI⁴

^{1,4} School of Mechanical Engineering, College of Engineering, University of Tehran, Tehran, I. R. of Iran

² Mechanical Engineering Department, Babol University of Technology, Babol, I. R. of Iran

Email: afrasiab@nit.ac.ir

³ Center of Excellence in Design, Robotics, and Automation, Department of Mechanical Engineering, Sharif University of Technology, Azadi Ave., Tehran, I. R. of Iran

Abstract– In this paper, based on the slab method of analysis, a novel and general approach is developed for studying the radial forging process with curved profile dies. The presented approach is not only more general with respect to previous studies, but it is also easier to understand and use and can be efficiently used for optimization of the die profile depending on the forging geometry and conditions. The obtained general equations reduce to those obtained in previous studies for the special case of linear dies. The process is also simulated by the finite element method to further enhance the results of the study. The obtained results provide useful information for the optimal design of the radial forging die.

Keywords– Radial forging, slab method, finite element method, die profile design

1. INTRODUCTION

Radial forging is a modern and cost effective process used for precision forging of round and tubular components, with or without an internal profile. Components produced by radial forging typically have good mechanical and metallurgical properties including smooth surface finish, preferred fiber structure, minimum notch effect and increased material strength [1-3].

Deformation in radial forging results from a large number of short stroke and high speed pressing operations by four hammer dies, while work-piece rotates and axially advances between the dies after each blow. Dies are arranged radially around the work-piece, as shown in Fig. 1.

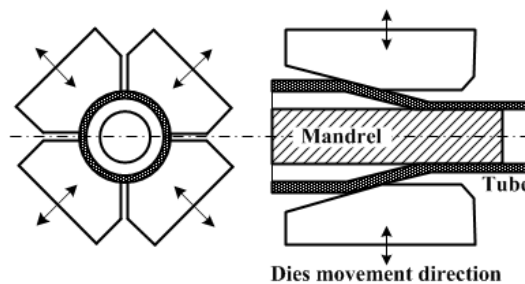


Fig. 1. Arrangement of dies

Among parameters affecting the deformation pattern and quality of the forged product, the die shape is of prime importance [1, 4, 5]. Generally, the die profile shape is made of two sections, the inlet section, which forms a conical surface and the die land, which is cylindrical, as shown in Fig. 2.

*Received by the editors March 10, 2014; Accepted June 18, 2014.

**Corresponding author

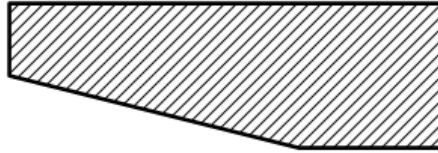


Fig. 2. A schematic side view of the radial forging die

Using slab method of analysis in [4], Ghaei et al. considered linear and circular (convex, concave and hybrid) profiles for the die inlet zone and studied the effects of the die shape on the deformation pattern and quality of radially forged products. In another study, Ghaei and Movahhedy [6] modeled the radial forging process by finite element method and studied the effect of the die shape in the cross-section area on the work-piece deformation. Using finite element analysis and microhardness test in [1], Sanjari et al. concluded that among dies with different linear and circular profiles, the die with a convex profile leads to a product with minimum inhomogeneity.

In the above-mentioned studies, the analyses were restricted to special, namely linear and circular, die profiles. However, here a generalized slab method analysis is presented that is capable of modeling the radial forging process with virtually any curved shape die profile. Finite element simulations are also performed to further examine the effect of the die profile on the process parameters.

This paper is organized as follows. The slab method formulation is developed in section 2. The modeling procedure is explained in section 3. The results of different analyses are presented and discussed in section 4. Finally, the concluding remarks are summarized in section 5.

2. THE SLAB METHOD ANALYSIS

As shown in Fig. 3, three distinct regions of deformation exist in the radial forging process: (1) sinking zone, (2) forging zone and (3) sizing zone. The sinking zone is a part of the conical region of the die in which the die contacts the outer surface of the tube, but the inner surface of the tube has not reached the mandrel yet. In this region, both the inner and outer diameter of the tube are reduced under the die pressure. In the forging zone, the inner diameter of the tube has reached the mandrel and thus only the outer diameter of the tube is changed under the die pressure. As a result, the material flows in the axial direction and the tube length increases. Most of the axial deformation happens in this region. In the sizing zone, both the inner and outer diameters have almost arrived at their final size and thus the deformation in this region is mostly elastic. The principle function of this region is to improve the finish quality of the inner surface.

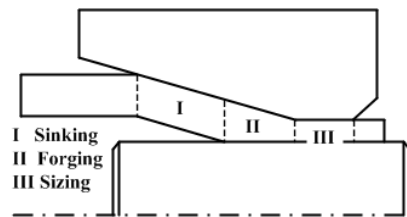


Fig. 3. Different deformation zones in the radial forging process

The following assumptions are made for the slab method analysis:

1. The tube thickness remains constant throughout the sinking zone.
2. Friction at the die-tube interface produces a constant friction shear stress.
3. The normal stress acting on the slab does not vary over the cross-section and it is also a principle stress.
4. The slab is free from shear stresses.
5. The material is rigid-perfectly plastic.

a) The sinking zone

Figure 4 shows the stresses acting on an element of material in the sinking zone. In order for the element to be in equilibrium, we must have:

$$(\sigma_1 + d\sigma_1)(A_1 + dA_1) - \sigma_1 A_1 - pA_2 \sin \alpha - \tau A_2 \cos \alpha = 0 \quad (1)$$

where σ_1 is the normal stress parallel to the die surface, A_1 and A_2 are the cross sectional and lateral area of the slab, p and τ are the radial pressure and shear stress due to friction, and α is the slab angle defined in Fig. 4.

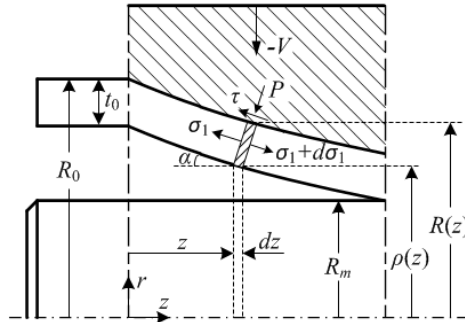


Fig. 4. Stresses acting on an element in the sinking zone

The following geometrical relations can be deduced from Fig. 4:

$$A_1 = \pi[R^2(z) - \rho^2(z)] \Rightarrow dA_1 = \pi[2R(z)R'(z)dz - 2\rho(z)\rho'(z)dz] \quad (2)$$

$$A_2 = 2\pi R(z) \frac{dz}{\cos \alpha}$$

The ‘ ’ symbol in this equation represents the first derivative with respect to z , ρ is the slab inner radius and R is its outer radius. Substituting Eq. (2) into Eq. (1) yields:

$$\begin{aligned} & \sigma_1 \times 2\pi[R(z)R'(z)dz - \rho(z)\rho'(z)dz] + d\sigma_1 \times \pi[R^2(z) - \rho^2(z)] \\ & - p[2\pi R(z) \frac{dz}{\cos \alpha}] \sin \alpha - \tau[2\pi R(z) \frac{dz}{\cos \alpha}] \cos \alpha = 0 \end{aligned} \quad (3)$$

which can be simplified to:

$$\begin{aligned} & 2\sigma_1[R(z)R'(z)dz - \rho(z)\rho'(z)dz] + d\sigma_1[R^2(z) - \rho^2(z)] \\ & - 2pR(z) \tan \alpha dz - 2\tau R(z) dz = 0 \end{aligned} \quad (4)$$

Also from the geometry in Fig. 4, we can write:

$$\tan \alpha = -R'(z) \quad (5)$$

This reduces Eq. (4) to:

$$\frac{d\sigma_1}{dz} = \frac{-2\sigma_1[R(z)R'(z) - \rho(z)\rho'(z)] - 2pR(z)R'(z) + 2\tau R(z)}{[R^2(z) - \rho^2(z)]} \quad (6)$$

Next, we consider equilibrium of the element in the slab radial direction to obtain (see Fig. 5):

$$\frac{P}{\sigma_3} = -\frac{R(z) - \rho(z)}{R(z)} \quad (7)$$

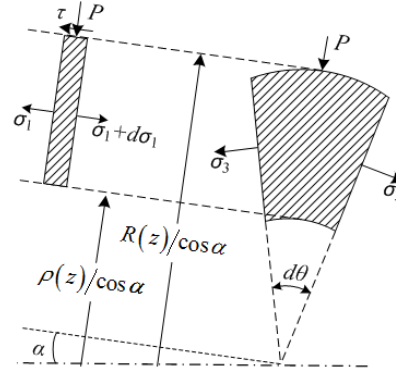


Fig. 5. Free body diagram of an element in the sinking zone

Where σ_3 is the hoop stress on the slab as shown in Fig. 5. In the sinking region, the radial pressure on the die is small compared with the principal longitudinal and circumferential stresses, and therefore the approximate yield condition is given by:

$$\sigma_1 - \sigma_3 = \bar{\sigma} \quad (8)$$

where $\bar{\sigma}$ is the yield stress of the workpiece material. Solving Eqs. (7) and (8) for p yields:

$$p = (\bar{\sigma} - \sigma_1) \frac{R(z) - \rho(z)}{R(z)} \quad (9)$$

Substituting p from Eq. (9) into Eq. (6) gives:

$$\frac{d\sigma_1}{dz} = \frac{2\sigma_1\rho(z)[\rho'(z) - R'(z)]}{[R^2(z) - \rho^2(z)]} - \frac{2\bar{\sigma}R'(z)[R(z) - \rho(z)]}{[R^2(z) - \rho^2(z)]} + \frac{2\tau_1R(z)}{[R^2(z) - \rho^2(z)]} \quad (10)$$

Using the reasonable assumption that the inner profile of the tube $\rho(z)$ is parallel to its outer profile $R(z)$, we will have:

$$R'(z) = \rho'(z) \quad (11)$$

Substituting Eq. (11) into Eq. (10) gives:

$$\frac{d\sigma_1}{dz} = -\frac{2\bar{\sigma}R'(z)[R(z) - \rho(z)]}{[R^2(z) - \rho^2(z)]} + \frac{2\tau R(z)}{[R^2(z) - \rho^2(z)]} \quad (12)$$

In the analysis of the radial forging process, it is normally assumed that the frictional shear stress varies according to the sticking condition [4, 6, 7]:

$$\tau = \frac{m\bar{\sigma}}{\sqrt{3}} \quad (13)$$

where m is the constant friction factor. Applying this assumption to Eq. (12) leads to:

$$\frac{d\sigma_1}{dz} = -\frac{2\bar{\sigma}R(z)}{[R^2(z) - \rho^2(z)]} \left(\frac{R'(z)[R(z) - \rho(z)]}{R(z)} - \frac{m}{\sqrt{3}} \right) \quad (14)$$

This equation gives the variation of the axial stress σ_1 in the sinking zone with respect to the axial distance z . Using the derivative chain rule, we can write:

$$\frac{d\sigma_1}{dR} = \frac{1}{R'(z)} \frac{d\sigma_1}{dz} \quad (15)$$

Therefore, the σ_1 variation along the radial distance R is as follows:

$$\frac{d\sigma_1}{dR} = -\frac{2\bar{\sigma}R}{R[R^2 - \rho^2]} \left(\frac{R'[R - \rho]}{R} - \frac{m}{\sqrt{3}} \right) \quad (16)$$

Equation (16) holds for a die that has a general curved shape profile. In the special case of the linear die with the inlet angle of α , we have:

$$R' = -\tan \alpha \quad (17)$$

Since the tube thickness t_0 is assumed constant in the sinking zone, for a linear die we can write:

$$\begin{aligned} R - \rho &= t_0 \cos \alpha \\ R^2 - \rho^2 &= t_0 \cos \alpha (2R - t_0 \cos \alpha) \end{aligned} \quad (18)$$

Substituting Eqs. (17) and (18) into Eq. (16) gives:

$$\frac{d\sigma_1}{dR} = \frac{2\bar{\sigma}R}{t_0(2R - t_0 \cos \alpha)} \left(-\frac{t_0}{R} - \frac{m}{\sqrt{3} \sin \alpha} \right) \quad (19)$$

which is the equation obtained previously by Lahoti and Altan in [7].

The corresponding radial pressure in the sinking zone is obtained by using Eq. (9).

b) The forging zone

According to Fig. 6, the force equilibrium of an element in the forging zone requires that:

$$(\sigma_z + d\sigma_z)(A_z + dA_z) - \sigma_z A_z - p_1 A_r \sin \alpha - \tau_1 A_r \cos \alpha - \tau_2 A_m = 0 \quad (20)$$

where σ_z is the axial stress, A_z and A_r are the cross sectional and lateral area of the slab, p_1 and τ_1 are the radial pressure and shear stress due to friction on the die-workpiece interface and τ_2 is the shear stress due to friction on the mandrel-workpiece interface. This can be simplified to:

$$\sigma_z dA_z + d\sigma_z A_z - p_1 A_r \sin \alpha - \tau_1 A_r \cos \alpha - \tau_2 A_m = 0 \quad (21)$$

where:

$$\begin{aligned} A_z &= \pi[R^2(z) - R_m^2] \Rightarrow dA_z = 2\pi R(z)R'(z)dz \\ A_r &= 2\pi R(z) \frac{dz}{\cos \alpha} \\ A_m &= 2\pi R_m dz \end{aligned} \quad (22)$$

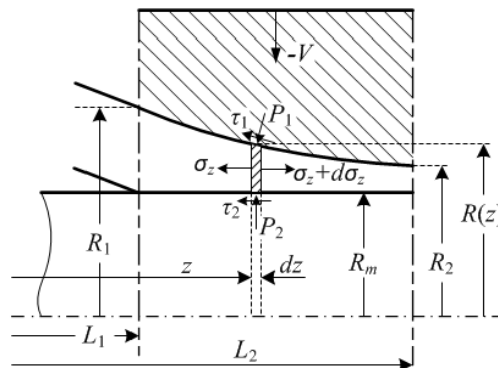


Fig. 6. Stresses acting on an element in the forging zone

in which R_m is the mandrel radius. Substituting Eq. (22) into Eq. (21) gives:

$$\begin{aligned} & \sigma_z \times 2\pi R(z)R'(z)dz + d\sigma_z \times \pi[R^2(z) - R_m^2] \\ & - p_1[2\pi R(z)\frac{dz}{\cos\alpha}] \sin\alpha - \tau_1[2\pi R(z)\frac{dz}{\cos\alpha}] \cos\alpha - \tau_2[2\pi R_m dz] = 0 \end{aligned} \quad (23)$$

which is simplified to:

$$\begin{aligned} & 2\sigma_z R(z)R'(z)dz + d\sigma_z[R^2(z) - R_m^2] \\ & - 2p_1 R(z) \tan\alpha dz - 2\tau_1 R(z)dz - 2\tau_2 R_m dz = 0 \end{aligned} \quad (24)$$

Also, from the geometry shown in Fig. 6, it follows that:

$$\tan\alpha = -R'(z) \quad (25)$$

Substituting this relation into Eq. (24) yields:

$$\frac{d\sigma_z}{dz} = \frac{-2\sigma_z R(z)R'(z) - 2p_1 R(z)R'(z) + 2\tau_1 R(z) + 2\tau_2 R_m}{[R^2(z) - R_m^2]} \quad (26)$$

Now, we consider the equilibrium of the element in the radial direction. According to Fig. 7, the following relationship is obtained:

$$\sigma_\theta[R(z) - R_m] = \sigma_{r1}R(z) - \sigma_{r2}R_m \quad (27)$$

Where σ_{r1} and σ_{r2} are radial stresses at the die and mandrel surfaces, respectively, and σ_θ is the circumferential stress.

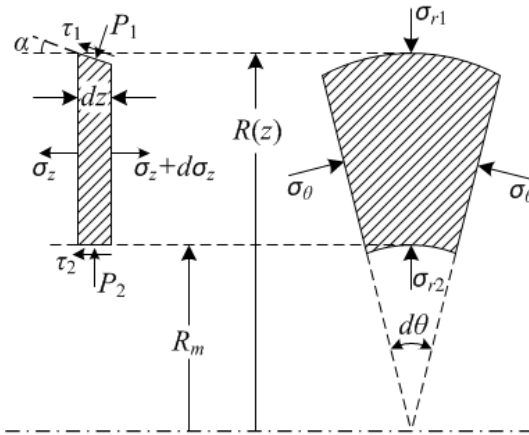


Fig. 7. Free body diagram of an element in the forging zone

By neglecting the radial stress variation through the element, we can assume that:

$$\sigma_{r1} = \sigma_{r2} = \sigma_r \quad (28)$$

Applying Eq. (28) to Eq. (27) results in:

$$\sigma_\theta[R(z) - R_m] = \sigma_r[R(z) - R_m] \Rightarrow \sigma_\theta = \sigma_r \quad (29)$$

Therefore, the yield condition in the forging zone becomes:

$$\sigma_z - \sigma_r = \bar{\sigma} \quad (30)$$

Considering the stress boundary condition at the tube-die interface yields:

$$p_1 = -\sigma_r - \tau_1 R'(z) \quad (31)$$

Substituting σ_r from Eq. (30) into Eq. (31), the following relationship is obtained:

$$p_1 = (\bar{\sigma} - \sigma_z) - \tau_1 R'(z) \quad (32)$$

Using this equation, Eq. (26) changes to:

$$\frac{d\sigma_z}{dz} = \frac{1}{[R^2(z) - R_m^2]} \{-2\bar{\sigma}R(z)R'(z) + 2\tau_1 R(z)[1 + R'^2(z)] + 2\tau_2 R_m\} \quad (33)$$

Assuming constant friction factor at the tube-die and tube-mandrel interfaces gives:

$$\tau_1 = \frac{m_1 \bar{\sigma}}{\sqrt{3}}, \quad \tau_2 = \frac{m_2 \bar{\sigma}}{\sqrt{3}} \quad (34)$$

Applying this relation to Eq. (33), after some simplification, results in:

$$\frac{d\sigma_z}{dz} = \frac{2\bar{\sigma}R(z)}{[R^2(z) - R_m^2]} \left\{-R'(z) + \frac{m_1}{\sqrt{3}}[1 + R'^2(z)] + \frac{m_2}{\sqrt{3}} \frac{R_m}{R(z)}\right\} \quad (35)$$

This equation gives the variation of axial stress σ_z in the forging zone with respect to axial distance z . For obtaining the variation of axial stress σ_z along the radial distance R , the chain rule is used according to Eq. (15). This way, we will have:

$$\frac{d\sigma_z}{dR} = \frac{2\bar{\sigma}R}{R'[R^2 - R_m^2]} \left\{-R' + \frac{m_1}{\sqrt{3}}[1 + R'^2] + \frac{m_2}{\sqrt{3}} \frac{R_m}{R}\right\} \quad (36)$$

This equation holds for a die with an arbitrary curved shape profile. For the special case of linear dies, we use Eq. (17) to obtain:

$$\frac{d\sigma_z}{dR} = \frac{2\bar{\sigma}R}{-\tan \alpha [R^2 - R_m^2]} \left\{\tan \alpha + \frac{m_1}{\sqrt{3}}[1 + \tan^2 \alpha] + \frac{m_2}{\sqrt{3}} \frac{R_m}{R}\right\} \quad (37)$$

Simplifying this equation, we get the result obtained previously by Lahoti and Altan in [7]:

$$\frac{d\sigma_z}{dR} = -\bar{\sigma} \left\{ \left(1 + \frac{m_1}{\sqrt{3}} \frac{[1 + \tan^2 \alpha]}{\tan \alpha}\right) \frac{2R}{[R^2 - R_m^2]} + \frac{m_2}{\sqrt{3} \tan \alpha} \frac{2R_m}{[R^2 - R_m^2]} \right\} \quad (38)$$

The radial pressure on the die surface is equal to radial stress σ_r :

$$p_{\text{Forging}} = \sigma_r = \sigma_z - \bar{\sigma} \quad (39)$$

c) The sizing zone

Only a small portion of the material is plastically deformed in the sizing zone. However, all the material is elastically deformed to the yield point. Thus, it will be assumed that the yield condition given by Eq. (30) is also satisfied in the sizing zone. Considering the equilibrium of forces acting on an element in the sizing zone gives (see Fig. 8):

$$\frac{d\sigma_z}{dz} - \frac{2}{\sqrt{3}} \bar{\sigma} \frac{(m_1 R_2 + m_2 R_2)}{(R_2 + R_m) t_1} = 0, \quad L_2 \leq z \leq L_3 \quad (40)$$

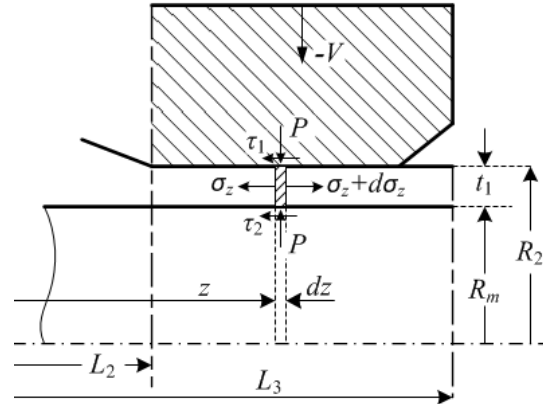


Fig. 8. Stresses acting on an element in the sizing zone

Integrating Eq. (40) yields:

$$\sigma_z = \sigma_{ze} + \frac{2}{\sqrt{3}} \bar{\sigma} \frac{(m_1 R_2 + m_2 R_m)}{(R_2 + R_m) t_1} (z - z_e), \quad L_2 \leq z \leq L_3 \tag{41}$$

where $\sigma_z = \sigma_{ze}$ at $z = z_e$.

When $z_e = L_3$ we have $\sigma_{ze} = \sigma_f$, where σ_f is the front pull per unit area, and when $z_e = L_2$, σ_{ze} is the axial stress obtained from the analysis of the forging zone.

Using Eq. (30), the radial pressure in the sizing zone is:

$$p_{Sizing} = \bar{\sigma} - \sigma_z \tag{42}$$

3. FINITE ELEMENT MODELING PROCEDURE

If we ignore the small gap between dies at the end of their stroke, the tube loadings and boundary conditions may be a function of r and z only (and not a function of θ). This means that the problem can be modeled as axisymmetric to reduce the computational time. The finite element analyses were performed using a verified FEM code previously used in [1, 4, 6, 8]. Since the deflection of the die and mandrel is very small compared to that of the deforming tube, it is accurate enough to assume that they are rigid bodies. The material was assumed to be perfectly plastic with a yield point of $\bar{\sigma} = 120$ MPa [4]. To model the friction in the contact surfaces, the penalty formulation was used. The limiting shear stress was obtained by $m\bar{\sigma}/\sqrt{3}$, where $m = 0.15$ is the constant friction factor commonly used for cold forging conditions [7]. The process parameters, including tube, die and mandrel geometry are presented in Table 1.

Table 1. Tube, die and mandrel geometry (mm)

Outer radius of the preform	100
Thickness of the preform	7
Outer radius of the product	90
Thickness of the product	4
Length of the die inlet	71
Length of the die land	10
Radius of the mandrel	86

4. RESULTS

a) Comparison of finite element and slab method results

The slab method equations obtained in Sec. 2 were solved numerically using an algorithm based on the Runge-Kutta scheme. Figure 9 compares the radial pressure distribution obtained by the slab method and the finite element analysis for a linear die with inlet angle of 8° .

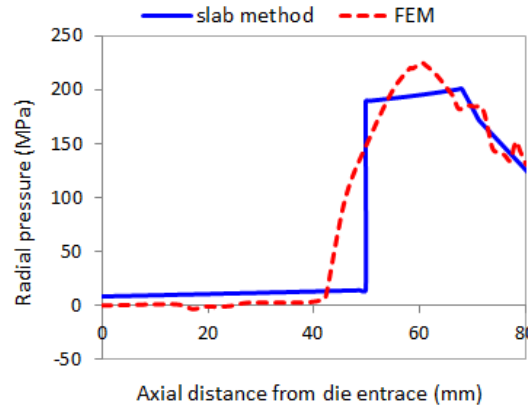


Fig. 9. Comparison of the results of slab method and FEM

The difference between pressures in the sinking zone stems from the bending of the tube in the die inlet that is not considered in the slab method [4]. In practice, during the dies impact, the tube is bent a little and the material is entered to the sinking zone. However, in the slab method analysis, it was assumed that the material flows sharply to the sinking zone. This bending causes an easier material flow to the sinking zone and less radial pressure at this zone as predicted by the finite element analysis. Another source of discrepancy between FEM and slab method results can be attributed to the changes in the radial pressure along the thickness of the tube that was assumed to be constant in the slab method analysis [4].

b) Effect of the die profile shape on the product quality

In order to study the effect of the die profile shape on the product quality, three different profiles were considered for the die, namely linear, quadratic and cubic order profiles, as shown in Figs. 10, 11 and 12, respectively.

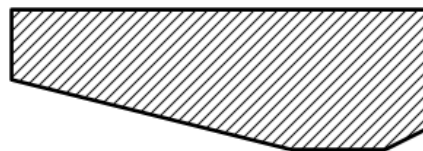


Fig. 10. Die with linear profile

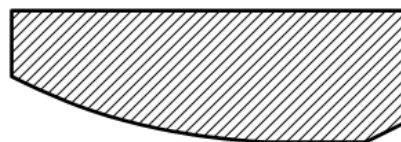


Fig. 11. Die with quadratic (2nd order) profile

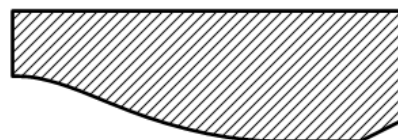


Fig. 12. Die with cubic (3rd order) profile

In the case of curved shape dies, to achieve a more homogenous structure in the product, it is recommended to use a profile in which the slope gradually changes to zero (equal to the slope of the sizing zone) at the end of forging zone [4]. Therefore, the two employed curved profiles are chosen to satisfy this recommendation.

The residual stress distribution was selected as the measure of the product quality since it is an indication of the degree of the deformation homogeneity. In other words, the more homogenous the deformation, the smaller the residual stress [6]. Furthermore, tensile residual stresses may lead to the opening of cracks which accelerates the failing of the tube while compressive stresses close the cracks and increase the tube life. Moreover, these stresses have a fundamental effect on the dimensional stability, wear resistance and fatigue life of the tube and are treated as one of the most important parameters of the surface quality.

Figure 13 compares the finite element solution for the residual Von-Mises stress distribution, i.e. the stress distribution after completion of the entire radial forging process [9] in the inner surface of the tube for different die profiles. As this figure shows, the tube tensile residual stress is minimum for the die with the quadratic profile while it is maximum for the die with the linear profile. Furthermore, the tube residual stress distribution is more uniform for dies with curved shape profiles. In these cases, the gradual change of the profile slope leads to more steady and homogenous deformation and flow of the tube between the die and mandrel, producing more favorable residual stress distribution in the tube.

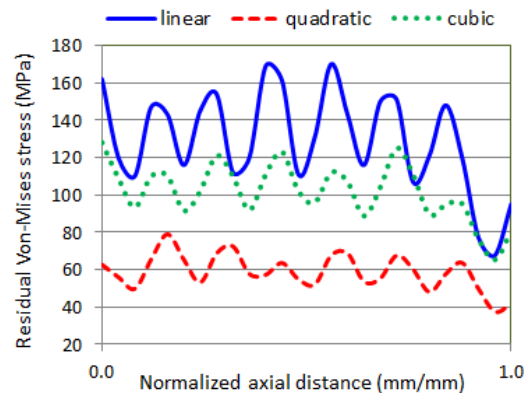


Fig. 13. Residual stress distribution for different die profiles

b) Effect of the die profile shape on the radial pressure distribution

Figure 14 shows the radial pressure distribution along the forging axis for the three different die profile shapes.

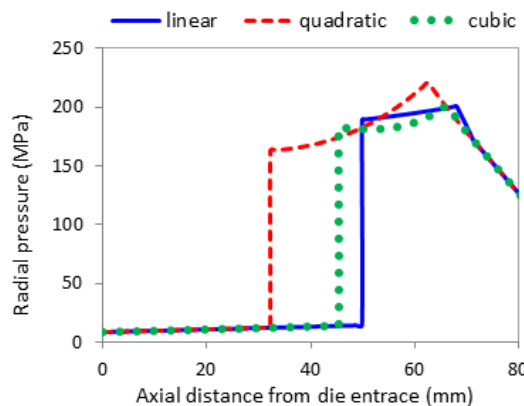


Fig. 14. Effect of the die profile shape on the radial pressure distribution

As illustrated in this figure, the die with quadratic order profile creates the largest radial pressure and consequently requires the largest forging force and energy. Furthermore, the position of the neutral plane moves towards the preform in this case. Therefore, either smaller axial force feed or smaller reduction in area should be considered in order to prevent overloading of machine.

On the other hand, the cubic order curve creates a smaller radial pressure on the die while the position of the neutral plane does not change significantly in this case compared with the linear die. Since the product quality (the residual pressure distribution shown in Fig. 13) is also desirable for the cubic order profile, it may be an optimal option for the radial forging die. It is to be noted that while finding the most optimal die profile is not the concern of this paper, the relations obtained in Section 2 can be easily used for further optimization of the die profile shape depending on the forging geometry and conditions.

5. CONCLUSION

The slab method of analysis was used to investigate the radial forging of tubes with curved profile dies. The presented approach is not only more general with respect to previous studies, but it is also easier to understand and use and can be efficiently used for optimization of the die profile depending on the forging geometry and conditions. The obtained general equations reduce to those obtained in previous studies for the special case of linear dies. Good agreement was observed between the results of the slab method and finite element analysis. It was shown that, the die with quadratic order profile provides the best residual stress distribution compared with the linear and cubic order dies, but it requires the largest forging force and energy. The cubic order die, on the other hand, provides a good residual stress distribution in the product and requires a smaller force and energy.

REFERENCES

1. Sanjari, M., Saidi, P., Karimi Taheri, A. & Hossein-Zadeh, M. (2012). Determination of strain field and heterogeneity in radial forging of tube using finite element method and microhardness test. *Materials and Design*, Vol. 38, pp. 147–153.
2. Sahoo, A. K., Tiwari, M. K. & Mileham, A. R. (2008). Six sigma based approach to optimize radial forging operation variables. *Journal of Materials Processing Technology*, Vol. 202, pp. 125–136.
3. Sanjari, M., Karimi Taheri, A. & Ghaei, A. (2007). Prediction of neutral plane and effects of the process parameters in radial forging using an upper bound solution. *Journal of Materials Processing Technology*, Vol. 186, pp. 147–153.
4. Ghaei, A., Movahhedy, M. R. & Karimi Taheri, A. (2005). Study of the effects of die geometry on deformation in the radial forging process. *Journal of Materials Processing Technology*, Vol. 170, pp. 156–163.
5. Khaleed, H. M. T., Samad, Z., Mujeebu, M. A., Badaruddin, A., Badruddin, I. A., Abdullah, A. B. & Salman Ahmed, N. J. (2012). *FEM simulation and experimental validation of flash-less cold forging for producing AUV propeller blade*. *Iranian Journal of Science and Technology, Transactions of Mechanical Engineering*, Vol. 36, No. M1, pp. 1-12.
6. Ghaei, A. & Movahhedy, M. R. (2007). Die design for the radial forging process using 3D FEM. *Journal of Materials Processing Technology*, Vol. 182, pp. 534–539.
7. Lahoti, G. D. & Altan, T. (1976). Analysis of the radial forging process for manufacturing of rods and tubes. *Journal of Engineering for Industry*, Vol. 98, pp. 265-271.

8. Ghaei, A., Movahhedy, M. R. & Karimi Taheri, A. (2008). Finite element modelling simulation of radial forging of tubes without mandrel. *Materials and Design*, Vol. 29, pp. 867–872.
9. Jang, D. Y. & Liou, J. H. (1998). Study of stress development in axi-symmetric products processed by radial forging using a 3-D non-linear finite-element method. *Journal of Materials Processing Technology*, Vol. 74, pp. 74–82.